Beach recovery from extreme storm activity during the 2013-14 winter along the Atlantic coast of Europe

Dodet Guillaume [1, *], Castelle Bruno [2, 3], Masselink Gerd [4], Scott Timothy [4], Davidson Mark [4], Floc'h France [5], Jackson Derek [6], Suanez Serge [1]

[1] Univ Bretagne Occidentale, Inst Univ Europeen Mer, CNRS, UMR LETG 6554, Plouzane, France.
[2] CNRS, UMR EPOC, Pessac, France.
[3] Univ Bordeaux, UMR EPOC, Pessac, France.
[4] Plymouth Univ, Sch Biol & Marine Sci, Coastal Proc Res Grp, Plymouth, Devon, England.
[5] Inst Univ Europeen Mer UBO, CNRS, Geosci Ocean UMR 6538, Plouzane, France.
[6] Ulster Univ, Sch Geog & Environm Sci, Ctr Coastal & Marine Res, Coleraine, Londonderry, North Ireland.

* Corresponding author : Guillaume Dodet, email address : guillaume.dodet@univ-brest.fr

Abstract :

The storm sequence of the 2013-14 winter left many beaches along the Atlantic coast of Europe in their most eroded state for decades. Understanding how beaches recover from such extreme events is essential for coastal managers, especially in light of potential regional increases in storminess due to climate change. Here we analyse a unique dataset of decadal beach morphological changes along the west coast of Europe to investigate the post-2013-14 winter recovery. We show that the recovery signature is site specific and multi-annual, with one studied beach fully recovered after 2 years, and the others only partially recovered after 4 years. During the recovery phase, winter waves primarily control the timescales of beach recovery, as energetic winter conditions stall the recovery process whereas moderate winter conditions accelerate it. This inter-annual variability is well correlated with climate indices. On exposed beaches, an equilibrium model showed significant skill in reproducing the post-storm recovery and thus can be used to investigate the recovery process in more detail. (c) 2018 John Wiley & Sons, Ltd.

1. Introduction

Sand and gravel beaches may undergo dramatic erosion and recession during sequences of extreme storm wave events (Ferreira, 2006), leaving them in a state of morphological dis-equilibrium. A phase of 'recovery' towards pre-storm sediment volume is then a natural morphodynamic response to this depleted state (Brenner et al., 2018). Because the rates of recovery depend on the magnitude of the storm-induced changes, the subsequent hydrodynamic conditions, the sediment availability, and the geological setting, predicting the time until full recovery is achieved (if ever) is challenging. The current predictions of climate change indicate an acceleration of sea level rise (Cazenave and Cozannet, 2014) and a poleward shift of midlatitudes storms (Tamarin and Kaspi, 2017), which will likely increase extreme water levels (Vousdoukas et al., 2018) and winter wave intensity in several regions of the world, particularly in the southern hemisphere (Semedo et al., 2013). Hence, addressing the timescales of beach recovery to extreme storm winters, such as the 2013/14 winter, can provide a measure of coastal resilience in a changing climate.

Beach recovery from severe storms has been shown to spread over years to decades (Morton et al., 1994; Houser and Hamilton, 2009; Castelle et al., 2017a). Since beach morphodynamics are often characterized by a significant seasonal signal (Aubrey, 1979; Masselink and Pattiaratchi, 2001; Davidson and Turner, 2009), the long-term recovery signature is often hard to detect within the shorter-term fluctuations (Thom and Hall, 1991; Stephan et al., 2015). Therefore, high-frequency monitoring of beachmorphology over long time periods is crucial to understand better storm recovery (Turner et al., 2016). Unfortunately, such monitoring programmes are scarce, and the few available data sets have been used mostly to characterize extreme storm responses (Scott et al., 2016; Barnard et al., 2017), investigate the parameters controlling beach morphological changes (Yates et al., 2011) and develop semi-empirical equilibrium models able to reproduce these morphological changes (Davidson and Turner, 2009; Yates et al., 2009; Splinter et al., 2014). However, ongoing field monitoring programmes in France and UK have recently shed some lights on the key mechanisms involved during post-storm recovery (Scott et al., 2016; Castelle et al., 2017a; Burvingt et al., 2018). Scott et al. [2016], investigated the morphological changes at three contrasting sites in SW England during the two years that followed the extreme 2013/14 winter. They found that the recovery mechanisms and timescales were highly dependent on the site characteristics, and that high-energy wave events were essential for the recovery of sediments. Burvingt et al. (2018), found that for a number of very similar beaches in SW England, recovery from the 2013/14 storm was regionally-coherent, multi-annual (>3 years), and mainly controlled by winter-wave conditions. Castelle et al. (2017a) investigated how the beach-dune system of an exposed site in SW France recovered from winter 2013/14 and found that only after 1.5 year the beach-dune system almost fully recovered to its pre-winter volume. These site-specific recovery rates highlight the need to conduct studies at broader scales, including different beaches, in order toinvestigate the key parameters that control the recovery timescales.

During the 2013/14 winter, a highly unusual sequence of extratropical storms crossed the North-East Atlantic region. This winter was the most energetic winter along the Atlantic coast of Europe since at least 1948 (Masselink et al., 2016a), and most of the west European coastline was severely impacted (Castelle et al., 2015; Blaise et al., 2015; Masselink et al., 2016b; Autret et al., 2016). Although winter waves are known to be well correlated with the North Atlantic Oscillation (NAO) index at high latitudes (Bacon and Carter, 1993; Dodet et al., 2010; Bromirski and Cayan, 2015), this exceptional winter was not associated with a particularly high NAO. Castelle et al. (2017b) computed a new climate index based on the sea level pressure gradient between Ireland and the Canary Islands: the West Europe Pressure Anomaly (WEPA). They showed that the 2013/14 winter was associated with the highest WEPA over 1948-2016, which reflects an intensified and southward shift of the sea level pressure difference between the Icelandic low and the Azores high, driving severe storms that funnel high-energy waves toward western Europe southward of 52 °N. This high WEPA was linked to a recent increase in inter-annual variability, which was also observed in the winter-wave variability along western Europe (Castelle et al., 2018).

In this paper, we investigate the post-2013/14 winter recovery of five beaches along the west coast of Europe; these are the same beaches for which the 2013/14 storm response was reported in Masselink et al. (2016a). Our objectives are threefold: 1) to obtain insight into the time scale of recovery for this extreme event for the different locations; 2) to explain the difference in observed recovery time scales by identifying the key factors involved; and 3) to determine extent to which extreme erosion and recovery processes can be modeled using present equilibrium models.

2. Methods

2.1. Wave Modeling

Two wave model hindcasts were used in this study. First, a large-scale and low-resolution model was used to characterize the wave climate in the North-East Atlantic, and more particularly the N-S differences in the wave forcing along the west coast of Europe. For this purpose, the spectral wave model WAVEWATCH III V4.18 (WW3, Tolman, 2014) was implemented on a 0.5 ° resolution grid covering the North Atlantic Ocean and forced with the 6-hourly wind fields of the NCEP/NCAR Global Reanalysis Project (Kalnay et al., 1996) from January 1948 to December 2017. Time series of significant wave heights (H_s) were extracted at three deep-water locations (shown in Figure 1): north west of Ireland (10.0 °W ; 56.0 °N), in the Bay of Biscay (7.0 °W ; 47.0 °N), and west of Portugal (11.0 °W ; 40.0 °N). Details of the model setup and validation of the simulations with wave buoy observations can be found in itetmasselink-extreme-2016-1. Second, a smaller scale, high-resolution model was used to simulate the wave conditions close to the breaking point at each study site. Indeed, the offshore wave conditions simulated with the 0.5 ° model were not necessarily representative of nearshore wave conditions at some of the sheltered study locations. For this purpose we used a WW3 hindcast (1992-2017) implemented on an unstructured grid with a resolution increasing from 10 km offshore to 200 m in the coastal region extending from north of Spain to south of Ireland (Boudière et al., 2013). This model has been extensively validated with directional buoy and satellite altimeter and showed excellent skill, with correlation coefficients of morethan 0.94 and root-mean square errors less than 0.2 m for the whole set of validation points (Boudière et al., 2013; Ardhuin et al., 2012). Model outputs were extracted for each study site at a distance less than 6 km from the coast, in water depths of 20-35 m. Seasonal means were computed for the winter (DJFM) and for the

spring-summer-autumn (AMJJASON).

2.2. Study Sites and Beach Volumes

Five beaches along the Atlantic coast of Europe were surveyed on a monthly basis for more than 10 years. This data set represents one of the most complete series of beach profiles along western Europe. The location of the study beaches are shown in Figure 1, and the morphological characteristics of the study sites are given in Table 1. Additional information on the survey methods can be found in Masselink et al. (2016a). Since Slapton Sands displayed a strong alongshore variability in beach profile evolution, two representative beach profiles were analyzed separately, corresponding to the middle (SP10) and northern end (SP18) of the beach.

The extension of this data set to November 2017 was used to investigate the morphological recovery of the beaches four years after the exceptionnal 2013/14 winter. For this purpose, the beach volume above mean sea level (V) was computed for each site, with no upper limit set except at Perranporth where data was not collected for elevations higher than 3 m above MSL. Beach volume V, which therefore includes the dune system at Vougot, Porsmilin and Truc Vert, was assumed to provide an accurate and integrated measure of the beach system change (see left-hand panels of Fig. 4 in Masselink et al. (2016a)). Note that the upper beach of Porsmilin is topped by an artificial embankment that culminates at 6.2 m above MSL. Then, thebeach volume changes ($|dV|$) were divided into four components: 1) beach volume change caused by the long-term trend computed over the period prior to the 2013/14 winter; 2) seasonal signal, computed from the detrended signal as the average annual difference between the maximum and minimum beach volume ($\frac{1}{N}\sum_{i=1}^{N}|V_{i,max} - V_{i,min}|$, where i is a yearly increment and N is the number of years in the time series); 3) 2013/14 winter response, computed as the difference in beach volume prior to and after the 2013/14 winter; and 4) post-2013/14 winter recovery, computed as the difference in beach volumes between April 2014 and November 2017. Note that the long-term trend and the seasonal contribution were only computed over the time period prior to the 2013/14 winter to ensure these signals were not affected by the 2013/14 winter storm response. Rates of beach volume changes (dV/dt) were computed for the winter and spring-summer-autumn from the observations closest in time to December 1 and April 1. When no observations were available within two weeks before or after these dates, the corresponding dV/dt was not computed. In the remaining of the paper, the percentage of recovery is computed as the beach volume change associated with the post-storm recovery relative to the beach volume change associated with the 2013/14 winter response, as defined above (components 3 and 4).

2.3. Beach Equilibrium Modeling

To assess whether an equilibrium-based model can be used to forecast beach recovery to an extreme storm event, the ShoreFor model (Davidson et al., 2013) was applied. This semi-empirical model predicts beachface erosion when the wave conditions are more energetic than the equilibrium conditions (computed as a weighted average of past wave conditions) and vice-versa, and the magnitude of change is proportional to the incident wave power and degree of disequilibrium. The model has two free parameters that require calibration: a disequilibrium term and a linear trend term. The linear trend-term crudely accounts for all processes other than wave-driven cross-shore transport, including longshore sediment transport processes. The reader is referred to Davidson et al. (2013) for a full description of the model. For all sites, the model was calibrated wth the period of observations prior to the 2013/14 winter, and validated during the remaining period that includes the 2013/14 winter storm response and the

subsequent 4-year recovery period. The model skill was assessed with the correlation coefficient (R) between observed (x) and simulated (x_m) beach volumes, the root-mean-square error ($RMSE$), and the root-mean-square error normalized by the observed variance prior to the 2013/14 winter ($NRMSE$). Because records with a significant linear trend, possibly induced by longshore transport processes or other net source/sinks of sediments, sometimes showhigh model skill solely attributable to the linear trend component in the model, the model skill was also assessed using the Brier Skill Score (BSS), which allows comparison of the model residuals with a suitable baseline (x_b), taken here as the linear trend component of the model. The BSS is computed as follows:

$$BSS = 1 - \frac{\sum (x - x_m)^2}{\sum (x - x_b)^2} \tag{1}$$

A positive BSS indicates an improvement relative to the baseline, and values greater than 0.0, 0.3, 0.6, 0.8 are typically described as 'poor', 'fair', 'good', 'excellent', respectively (van Rijn et al., 2003; Sutherland et al., 2004). Note that this modelling approach does not resolve long-shore transport processes and is thus expected to show poor skills when applied to environments dominated by long-shore transport.

3. Results

3.1. Modeled Wave Conditions

The wave conditions simulated with the regional model over the period 2002-2017 for the north-west of Ireland, the Bay of Biscay, and west of Portugal are shown in Figure 1. A clear seasonal signal characterizes the three time series, with winter-mean H_s much larger than spring-summer-autumn-mean H_s (56 % greater on average, and up to 120 % greater locally). Moreover, the winter-mean values display strong inter-annual variability ($\sigma/\overline{H_s} = 0.12$ on average, where σ is the standard deviation, and $\overline{H_s}$ is the long-term mean H_s), whereas the spring-summer-autumn-mean values display much lower inter-annual variability ($\sigma/\overline{H_s} = 0.06$). The consequence of these fluctuations is that, contrary to spring-summer-autumn means, the winter-mean H_s may differ significantly from one year to another. For instance, the largest winter-mean H_s in the Bay of Biscay and west of Portugal occurred during the 2013/14 winter, and they were approximately 35 % greater than the long-term mean winter H_s. During the following winter, wave conditions were moderate in the Bay of Biscay and west of Portugal, but obtained their maximum north of Ireland. These trendswere inverted during the 2015/16 winter as the winter-mean H_s was very large in the Bay of Biscay and west of Portugal, but moderate north of Ireland. The most recent 2016/17 winter was moderate in all three regions. This inter-annual variability of winter-mean H_s was shown to be significantly correlated with the WEPA index southward of 52 °N (Castelle et al., 2017b) and with the NAO index further north (Bacon and Carter, 1993; Dodet et al., 2010; Bromirski and Cayan, 2015). This dependence on NAO and WEPA indices is confirmed by our results, with the highest (respectively lowest) NAO during the 2014/15 (respectively 2009/10) winter correlating with the maximum (respectively minimum) H_s north of Ireland for this winter, and the two highest WEPA during the 2013/14 and 2015/16 winters correlating with the maximum H_s in the Bay of Biscay and west of Portugal for these winters. Correlation coefficients between the winter-mean H_s and the NAO and WEPA indicesare shown on Figure 1.

3.2. Beach Recovery from the 2013/14 winter

Figure 2 shows the complete time series of beach volume changes for the six beach profiles (left-hand column), and the relative contributions of the long-term trend, seasonal signal, 2013/14 winter response and post-2013/14 winter recovery (right-hand column). Contrasting behaviors are observed. First, the most exposed sites, Perranporth and Truc Vert, suffered unprecedented erosion during the 2013/14 winter. Yet, after two years, Truc Vert had fully recovered, while Perranporth had only recovered 70 % after four years. The major difference in these recovery rates occurred during the year 2015. From early February to mid-December 2015, the beach volumes at Truc Vert increased steadily and the beach recovered more than 80 % of the sediments lost during the 2013/14 winter within a span of 10 months (see Castelle et al., 2017a, for details). At Perranporth, the beach was in a recovery phase for a shorter period of time - from late-March to November 2015 - regaining only 40 % of the sediments lost during the 2013/14 winter. This contrasting response can be directly related to the difference in wave conditions in January, March, November and December 2015 that were particularly stormy at Perranporth (H_s was 60 % higher than the annual mean at Perranporth and only 30 % higher at TrucVert). Porsmilin was also in its most eroded state after the 2013/14 winter, but after two years the beach had recovered by almost 80 %. This fast recovery was fostered by the relatively calm wave conditions during the 2014/15 winter that did not cause much erosion at this sheltered site. The beach volumes at Vougot are dominated by a decreasing long-term trend. Although the coastal dune retreated by more than 5 mduring the 2013/14 winter, the sediment remained in the intertidal zone and the beach volume actually increased slightly. After four years, the dune had prograded back by approximately 3 m. At Slapton Sands, the central (*SP10*) and east (textitSP18) profiles showed opposite behaviors as a result of beach rotation processes. An additional factor that could explain the difference in recovery rates is the difference in tidal range. Large tidal range cause shorter time period during which sediment transport can contribute to accretion within the upper intertidal profile and subsequently longer morphological response times. However, no clear conclusion on this process was drawn from our data set, since both slow (Perranporth) and fast (Porsmilin) responses were observed on these macrotidal beaches.

To investigate the relationship between beach dynamics and incident wave conditions, the rates of beach volume changes (dV/dt) during the winter season and during the spring-summer-autumn season are compared to the respective seasonal wave energy anomalies, i.e., the deviation of the season-mean wave energy from the long-term (1992–2017) annual mean wave energy $\overline{E}$ (Figure 3). Overall, dV/dt displays much greater variability during the winter season than during the rest of the year. At Perranporth, Pormsilin and Truc Vert, the winter-mean variability of dV/dt is clearly controlled by the wave conditions ($0.58 < R^2 < 0.65$). The near-zero intercept of the linear trends indicates that the beach profile is close to equilibrium when the winter-mean E is close to the long-term yearly mean $\overline{E}$. Although winter wave conditions are associated mostly with erosive conditions, low winter-mean E can cause beach accretion. For instance, during the 2009/10 winter, the wave conditions were particularly calm north of 50 °N, due to a very low NAO and a modest WEPA, and the sand volume at Perranporth increased by 26 m ^{3}/m. For the spring-summer-autumn season, correlations between dV/dt and wave energy anomalies are much lower and mostly insignificant at the 95 % level. One reason is that dV/dt cannot progressively increase when E tends towards zero; very low energy waves contribute less to onshore sediment transport than low to moderate energy waves, hence limiting recovery (Hoefel and Elgar, 2003; Fernández-Mora et al., 2015). At Slapton Sands profiles SP10 and SP18, the winter-mean dV/dt is also strongly controlled by the wave conditions; however, the correlations have

opposite signs as a result of beach rotation. Wiggins et al. (2017) showed very high correlations between beach volume changesand the directional wave power at Slapton Sands, and the insignificant correlations for the spring-summer-autumn season are probably because the beach changes were mostly controlled by the wave direction and not by the wave energy. At Vougot, thereis no correlation between dV/dt and the wave conditions. Indeed, the behavior of the beach-dune system is severely impacted by the presence of a jetty at the north-eastern end of the beach. Since its construction in 1974 the beachhas continually lost sediment, independent of the wave conditions (Suanez et al., 2010).

Finally, the beach volume changes were compared with the results of the beach equilibrium model ShoreFor (Davidson et al., 2013) to assess the amount of variance attributable to cross-shore sediment transport and to antecedent wave conditions. Theanalysis described in the previous paragraph treats each year independently, while ShoreFor accounts for antecedent wave conditions. It is therefore expected to explain more of the variability in the beach volume at the cross-shore dominated beaches through the disequilibrium term than a simple model based on a linear correlation between dV/dt and the mean wave height. Figure 4 shows the observed versus simulated beach volume changes using the ShoreFor model, as well as the error metrics textitRMSE, *NRMSE*, *R*, and *BSS*. Inspection of this figure reveals that Perranporth and Truc Vert have low *NRMSE* (<5 %) and 'excellent' *BSS*, indicating that ShoreFor is able to reproduce fairly well the storm response and subsequent recovery, and this variance is mostly induced by cross-shore processes. With a *NRMSE* < 15 % and a 'fair' *BSS*, ShoreFor results are moderate, and beach volume changes at Porsmilin can also be considered as dominated by cross-shore processes. Conversely, the negative *BSS* scores at Slapton SP18 and Vougot indicate that the model performs worse than predictions based on the long-term trend only. At Slapton SP10, both *R* and the *BSS* are relatively high; however, the very large *NRMSE* (270.4 %) reveals that some significant processes are ignored by the model. Hence, different modelling approaches must be applied at Vougot and Slapton Sands to simulate volume changes, including extreme storm response and post-storm recovery.

4. Discussion and Conclusions

The analysis of decadal morphological changes of beaches along the Atlantic coast of Europe exposed to a pronounced seasonal wave climate revealed that the dynamics of beaches are controlled by processes operating over a variety of time scales. In decreasing order these time scales are: long-term trends (decade), post-storm recovery (years), seasonal changes (months), and storm response (days). Total beach dynamics represent the sum of these components and for different beaches the relative contribution of each of these components varies significantly, making beach volume predictions challenging and site-specific. Moreover, beach recovery is conventionally thought to be a process that occurs during the calm summer months. However, although beachesdo recover during the spring-summer-autumn period at modest and relatively steady rates (not much inter-annual variability), it is the energetic winter conditions that primarily control the time it takes for beaches to recover from extreme erosion. Highly energetic winters stall or even reverse the recovery process, whereas calm winters continue the recovery process. Therefore, climate indices such as NAO and WEPA, which are known to explain a significant part of the inter-annual variability of winter wave conditions in the North-East Atlantic (Dodet et al., 2010; Castelle et al., 2017b), are well correlated with the recovery process. For instance, the most exposed sites Perranporth and Truc Vert required calm winter conditions to recover from the 2013/14 winter erosion, which correspond to negative values of WEPA. This was the case for the 2014/15 and 2016/17 winters (Figure 1), during which these beaches showed relatively small rates of volume changes (Figure 3). The recovery

of these beaches could have been accelerated if the 2015/16 winter, which was characterized by a high WEPA value, had not caused severe erosion and slowed down the recovery process (Figure 3). At Slapton Sands, easterlies have been shown to foster beach recovery following storm erosion by (southwesterly) Atlantic storms, and these are promoted in this region by negative NAO values (Wiggins et al., 2017). The systematic positive NAO winters that followed the 2013/14 winter, and the prevailing southwesterly wave conditions, limited beach recovery at this site.

Predicting long-term beach morphological change is of great importance to coastal managers. While process-based morphodynamic modeling systems are valuable tools to simulate the morphological impact of single storm events (e.g. McCall et al., 2010; Almeida et al., 2017), their computational cost prevents their application to multi-annual or even inter-annual morphological changes. In contrast, beach equilibrium models are computationaly cheap and can be applied for investigating long-term morphological changes (e.g. Yates et al., 2011; Splinter et al., 2014). For cross-shore transport dominated sites, the ShoreFor model calibrated with topographic data prior to the winter 2013/14 and forced with nearshore wave conditions simulated with a high-resolution model showed significant skills in reproducing the strong erosion caused by the extreme 2013/14 winter and the recovery phase that followed at Truc Vert and Perranporth. Not surprisingly, ShoreFor shows poor skill at sites where longshore processes and resulting beach rotation signal dominate shoreline variability, i.e. at Vougot and Slapton. At Porsmilin, due to the low elevation of the artificial embankments at the top of the upper beach, a significant fraction of the sediment lost during the winter 2013/14 was deposited further inland during washover events. We believe this may explain why the model failed in reproducing accurately the volume changes during and after the winter. Semi-empirical models combining the equilibrium-based behaviour owing to variability in incident wave energy with longshore processes are scarce and still under development (Vitousek et al., 2017; Robinet et al., 2017). Although out of scope of this study, the further development of these models will extend the domain of applicability of shoreline change models, making it possible to address coastal vulnerability and resilience in the context of climate change. Mentaschi et al. (2017) analyzed projection of extreme wave energy fluxes under a high emission scenario (Representative Concentration Pathways 8.5) and showed a significant increase in the 100-year return level of wave energy fluxes for the southern hemisphere and for some regions of the northern hemisphere. It is very likely that such changes in the wave climate will significantly impact beach morphodynamics at both event scales (storm response) and long-term scales (post-storm recovery), which will require accurate predictions for implementing coastal adaptation strategies.

Acknowledgments

providing the wind field reanalysis and the wave hindcast, respectively. The topographic and wave data that were used for the analysis are provided as supplementary material of this paper.

References

[1] Almeida, L. P., Masselink, G., McCall, R., and Russell, P. (2017). Storm overwash of a gravel barrier: Field measurements and XBeach-G modelling. *Coastal Engineering*, 120:22–35.

[2] Ardhuin, F., Roland, A., Dumas, F., Bennis, A.-C., Sentchev, A., Forget, P., Wolf, J., Girard, F., Osuna, P., and Benoit, M. (2012). Numerical Wave Modeling in Conditions with Strong Currents: Dissipation, Refraction, and Relative Wind. *Journal of Physical Oceanography*, 42(12):2101–2120.

[3] Aubrey, D. G. (1979). Seasonal patterns of onshore/offshore sediment movement. *Journal of Geophysical Research: Oceans*, 84(C10):6347–6354.

[4] Autret, R., Dodet, G., Fichaut, B., Suanez, S., David, L., Leckler, F., Ardhuin, F., Ammann, J., Grandjean, P., Allemand, P., and Filipot, J.-F. (2016). A comprehensive hydro-geomorphic study of cliff-top storm deposits on Banneg Island during winter 2013–2014. *Marine Geology*, 382:37–55.

[5] Bacon, S. and Carter, D. J. T. (1993). A connection between mean wave height and atmospheric pressure gradient in the North Atlantic. *International Journal of Climatology*, 13(4):423–436.

[6] Barnard, P. L., Hoover, D., Hubbard, D. M., Snyder, A., Ludka, B. C., Allan, J., Kaminsky, G. M., Ruggiero, P., Gallien, T. W., Gabel, L., McCandless, D., Weiner, H. M., Cohn, N., Anderson, D. L., and Serafin, K. A. (2017). Extreme oceanographic forcing and coastal response due to the 2015–2016 El Niño. *Nature Communications*, 8:14365.

[7] Blaise, E., Suanez, S., Stephan, P., Fichaut, B., David, L., Cuq, V., Autret, R., Houron, J., Rouan, M., Floc'h, F., Ardhuin, F., Cancouet, R., Davidson, R., Costa, S., and Delacourt, C. (2015). Review of winter storms 2013-2014 on shoreline retreat dynamic on Brittany coast. *Geomorphologie : Relief, Processus, Environnement*, 21(3):267–292.

[8] Boudière, E., Maisondieu, C., Ardhuin, F., Accensi, M., Pineau-Guillou, L., and Lepesqueur, J. (2013). A suitable metocean hindcast database for the design of Marine energy converters. *International Journal of Marine Energy*, 3–4:e40–e52.

[9] Brenner, O. T., Lentz, E. E., Hapke, C. J., Henderson, R. E., Wilson, K. E., and Nelson, T. R. (2018). Characterizing storm response and recovery using the beach change envelope: Fire Island, New York. *Geomorphology*, 300:189–202.

[10] Bromirski, P. D. and Cayan, D. R. (2015). Wave power variability and trends across the North Atlantic influenced by decadal climate patterns. *Journal of Geophysical Research: Oceans*, 120(5):3419–3443.

[11] Burvingt, O., Masselink, G., Scott, T., Davidson, M., and Russell, P. (2018). Climate forcing of regionally-coherent extreme storm impact and recovery on embayed beaches. *Marine Geology*, 401:112–128.

[12] Castelle, B., Bujan, S., Ferreira, S., and Dodet, G. (2017a). Foredune morphological changes and beach recovery from the extreme 2013/2014 winter at a high-energy sandy coast. *Marine Geology*, pages 41–55.

[13] Castelle, B., Dodet, G., Masselink, G., and Scott, T. (2017b). A new climate index controlling winter wave activity along the Atlantic coast of Europe: the West Europe Pressure Anomaly. *Geophysical Research Letters*, page 2016GL072379.

[14] Castelle, B., Dodet, G., Masselink, G., and Scott, T. (2018). Increased Winter-Mean

Wave Height, Variability, and Periodicity in the Northeast Atlantic Over 1949–2017. *Geophysical Research Letters*, 45(8):3586–3596.

[15] Castelle, B., Marieu, V., Bujan, S., Splinter, K., Robinet, A., Sénéchal, N., and Ferreira, S. (2015). Impact of the winter 2013-2014 series of severe Western Europe storms on a double-barred sandy coast: Beach and dune erosion and megacusp embayments. *Geomorphology*, 238:135–148.

[16] Cazenave, A. and Cozannet, G. L. (2014). Sea level rise and its coastal impacts. *Earth's Future*, 2(2):15–34.

[17] Davidson, M., Splinter, K., and Turner, I. L. (2013). A simple equilibrium model for predicting shoreline change. *Coastal Engineering*, 73:191–202.

[18] Davidson, M. A. and Turner, I. L. (2009). A behavioral template beach profile model for predicting seasonal to interannual shoreline evolution. *Journal of Geophysical Research: Earth Surface*, 114(F1):F01020.

[19] Dodet, G., Bertin, X., and Taborda, R. (2010). Wave climate variability in the North-East Atlantic Ocean over the last six decades. *Ocean Modelling*, 31(3–4):120–131.

[20] Fernández-Mora, A., Calvete, D., Falqués, A., and de Swart, H. E. (2015). Onshore sandbar migration in the surf zone: New insights into the wave-induced sediment transport mechanisms. *Geophysical Research Letters*, 42(8):2014GL063004.

[21] Ferreira, O. (2006). The role of storm groups in the erosion of sandy coasts. *Earth Surface Processes and Landforms*, 31(8):1058–1060.

[22] Hoefel, F. and Elgar, S. (2003). Wave-Induced Sediment Transport and Sandbar Migration. *Science*, 299(5614):1885–1887.

[23] Houser, C. and Hamilton, S. (2009). Sensitivity of post-hurricane beach and dune recovery to event frequency. *Earth Surface Processes and Landforms*, 34(5):613–628.

[24] Kalnay, E., Kanamitsu, M., Kistler, R., Collins, W., Deaven, D., Gandin, L., Iredell, M., Saha, S., White, G., Woollen, J., Zhu, Y., Leetmaa, A., Reynolds, R., Chelliah, M., Ebisuzaki, W., Higgins, W., Janowiak, J., Mo, K. C., Ropelewski, C., Wang, J., Jenne, R., and Joseph, D. (1996). The NCEP/NCAR 40-Year Reanalysis Project. *Bulletin of the American Meteorological Society*, 77(3):437–471.

[25] Masselink, G., Castelle, B., Scott, T., Dodet, G., Suanez, S., Jackson, D., and Floc'h, F. (2016a). Extreme wave activity during 2013/2014 winter and morphological impacts along the Atlantic coast of Europe. *Geophysical Research Letters*, page 2015GL067492.

[26] Masselink, G. and Pattiaratchi, C. B. (2001). Seasonal changes in beach morphology along the sheltered coastline of Perth, Western Australia. *Marine Geology*, 172(3):243–263.

[27] Masselink, G., Scott, T., Poate, T., Russell, P., Davidson, M., and Conley, D. (2016b). The extreme 2013/14 winter storms: hydrodynamic forcing and coastal response along the southwest coast of England. *Earth Surface Processes and Landforms*, 41:378–391.

[28] McCall, R. T., Van Thiel de Vries, J. S. M., Plant, N. G., Van Dongeren, A. R., Roelvink, J. A., Thompson, D. M., and Reniers, A. J. H. M. (2010). Two-dimensional time dependent hurricane overwash and erosion modeling at Santa Rosa Island. *Coastal Engineering*, 57(7):668–683.

[29] Mentaschi, L., Vousdoukas, M. I., Voukouvalas, E., Dosio, A., and Feyen, L. (2017). Global changes of extreme coastal wave energy fluxes triggered by intensified teleconnection patterns. *Geophysical Research Letters*, 44(5):2416–2426.

[30] Morton, R. A., Paine, J. G., and Gibeaut, J. C. (1994). Stages and Durations of Post-Storm Beach Recovery, Southeastern Texas Coast, U.S.A. *Journal of Coastal Research*, 10(4):884–908.

[31] Robinet, A., Castelle, B., Idier, D., Marieu, V., and Harley, M. D. (2017). On a reduced-complexity shoreline model combining cross-shore and alongshore processes. In *Coastal Dynamics*, pages 1853–1862, Helsingor, Denmark.

[32] Scott, T., Masselink, G., O Hare, T., Saulter, A., Poate, T., Russell, P., Davidson, M., and Conley, D. (2016). The extreme 2013/2014 winter storms: Beach recovery along the southwest coast of England. *Marine Geology*, 382:224–241.

[33] Semedo, A., Weisse, R., Behrens, A., Sterl, A., Bengtsson, L., and GÃ¼nther, H. (2013). Projection of Global Wave Climate Change toward the End of the Twenty-First Century. *Journal of Climate*, 26(21):8269–8288.

[34] Splinter, K. D., Turner, I. L., Davidson, M. A., Barnard, P., Castelle, B., and Oltman-Shay, J. (2014). A generalized equilibrium model for predicting daily to interannual shoreline response. *Journal of Geophysical Research: Earth Surface*, 119(9):1936–1958.

[35] Stephan, P., Suanez, S., and Fichaut, B. (2015). Long, Mid and Short-Term Evolution of Coastal Gravel Spits of Brittany, France. In *Sand and Gravel Spits*, Coastal Research Library, pages 275–288. Springer Cham.

[36] Suanez, S., Cariolet, J.-M., and Fichaut, B. (2010). Monitoring of recent morphological changesof the dune of Vougot Beach (Brittany, France) using Differential GPS. *Shore and Beach*, 78(1):37–40.

[37] Sutherland, J., Peet, A. H., and Soulsby, R. L. (2004). Evaluating the performance of morphological models. *Coastal Engineering*, 51(8):917–939.

[38] Tamarin, T. and Kaspi, Y. (2017). The poleward shift of storm tracks under global warming: A Lagrangian perspective. *Geophysical Research Letters*, 44(20):10,666–10,674.

[39] Thom, B. and Hall, W. (1991). Behaviour of beach profiles during accretion and erosion dominated periods. *Earth Surface Processes and Landforms*, 16(2):113–127.

[40] Tolman, H. L. (2014). User manual and system documentation of WAVEWATCH III version 4.18. *NOAA/NWS/NCEP/MMAB Technical Note 316*, (276):194.

[41] Turner, I. L., Harley, M. D., Short, A. D., Simmons, J. A., Bracs, M. A., Phillips, M. S., and Splinter, K. D. (2016). A multi-decade dataset of monthly beach profile surveys and inshore wave forcing at Narrabeen, Australia. *Scientific Data*, 3:160024.

[42] van Rijn, L. C., Walstra, D. J. R., Grasmeijer, B., Sutherland, J., Pan, S., and Sierra, J. P. (2003). The predictability of cross-shore bed evolution of sandy beaches at the time scale of storms and seasons using process-based Profile models. *Coastal Engineering*, 47(3):295–327.

[43] Vitousek, S., Barnard, P. L., Limber, P., Erikson, L., and Cole, B. (2017). A model integrating longshore and cross-shore processes for predicting long-term shoreline response to climate change. *Journal of Geophysical Research: Earth Surface*, page 2016JF004065.

[44] Vousdoukas, M. I., Mentaschi, L., Voukouvalas, E., Verlaan, M., Jevrejeva, S., Jackson, L. P., and Feyen, L. (2018). Global probabilistic projections of extreme sea levels show intensification of coastal flood hazard. *Nature Communications*, 9(1):2360.

[45] Wiggins, M., Scott, T., Masselink, G., Russell, P., Castelle, B., and Dodet, G. (2017). The role of multi-decadal climate variability in controlling coastal dynamics: re-interpretation of the 'lost village of Hallsands'. pages 96–107, Helsingor.

[46] Yates, M. L., Guza, R. T., and O'Reilly, W. C. (2009). Equilibrium shoreline response: Observations and modeling. *Journal of Geophysical Research: Oceans*, 114(C9):C09014.

[47] Yates, M. L., Guza, R. T., O'Reilly, W. C., Hansen, J. E., and Barnard, P. L. (2011). Equilibrium shoreline response of a high wave energy beach. *Journal of Geophysical Research: Oceans*, 116(C4):C04014.

Table 1. Summary of beach site characteristics. $\tan\beta$ is the intertidal slope and MSR stands for mean spring tide range

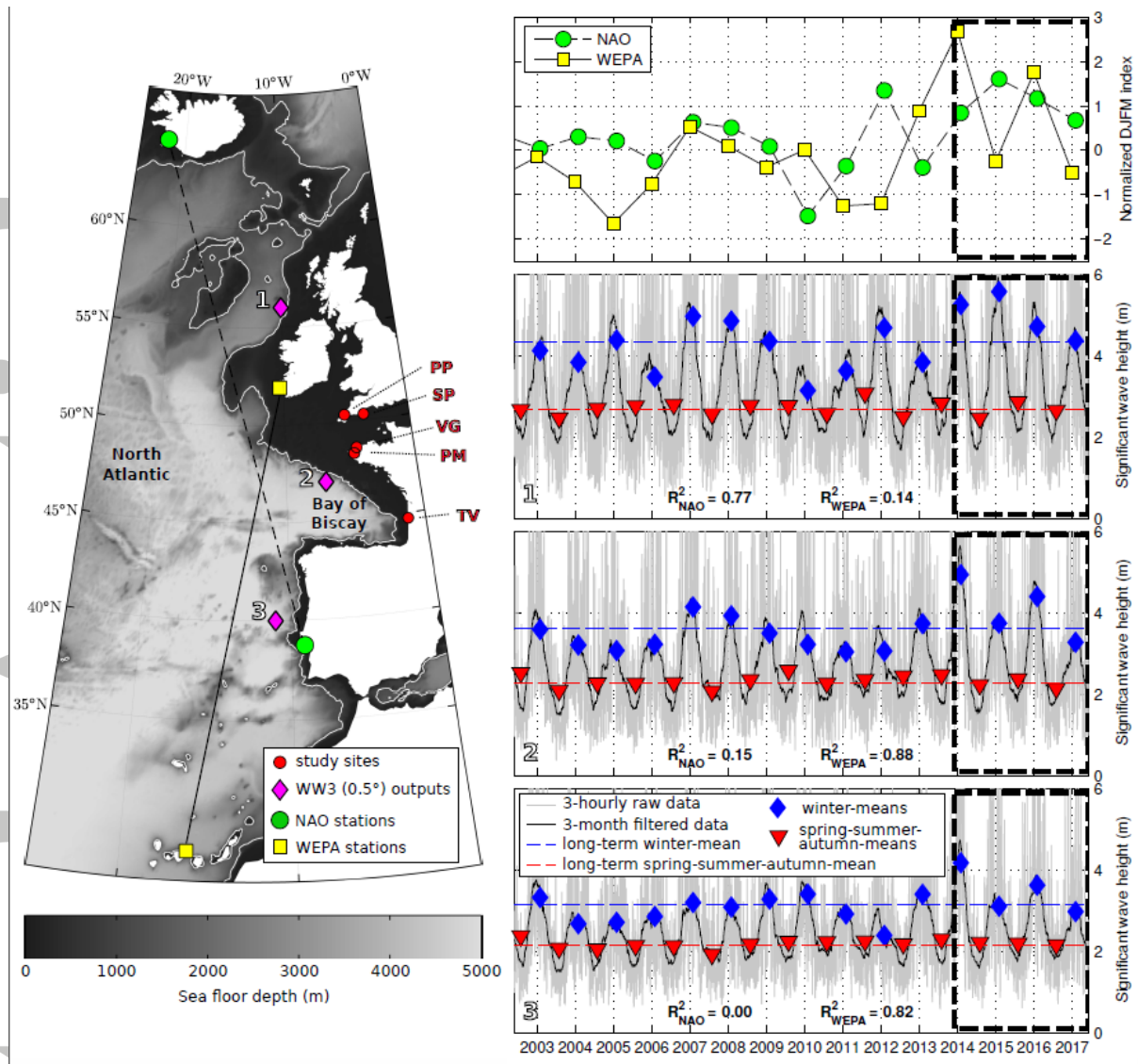| Name	Region	Exposure	Hinterland	D_{50} (mm)	$\tan\beta$	MSR (m)
Perranporth	Cornwall, UK	W Exposed	Dunes	0.35	0.015	4.5
Slapton	Devon, UK	SE Semi-sheltered	Lagoon	2-8	0.1	4.3
Vougout	Brittany, France	NNW Semi-exposed	Dunes	0.2-0.3	0.03	8.5
Porsmilin	Brittany, France	S Semi-shelterd	Seawall, Marsh	0.32	0.05	5.7
Truc Vert	Aquitaine, France	W Exposed	Dunes	0.4	0.025	3.9

Figure 1. (left) Location map of the Atlantic coast of Europe showing the offshore bathymetry (greyscale), virtual wave buoys (pink diamonds), beach study sites Perranporth (PP), Slapton Sands (SP), Vougot (VG), Porsmilin (PM), Truc Vert (TV) (red circles), and weather stations used to compute the NAO (green circles) and WEPA indices (yellow squares). The white contour line represents the 1000 m isobath. (right) Time series of NAO and WEPA indices (top panel), and time series of raw (grey line), 3-month filtered (black line), winter-mean (blue diamond) and spring-summer-autumn mean (red triangles) significant wave height at the virtual buoys 1, 2 and 3 (bottom 3 panels). The dashed rectangle indicates the 2013/14 winter and the 4-year recovery period that followed. Squared correlation coefficients (R^2) between winter-mean H_s and NAO and WEPA indices are provided for each virtual buoy.
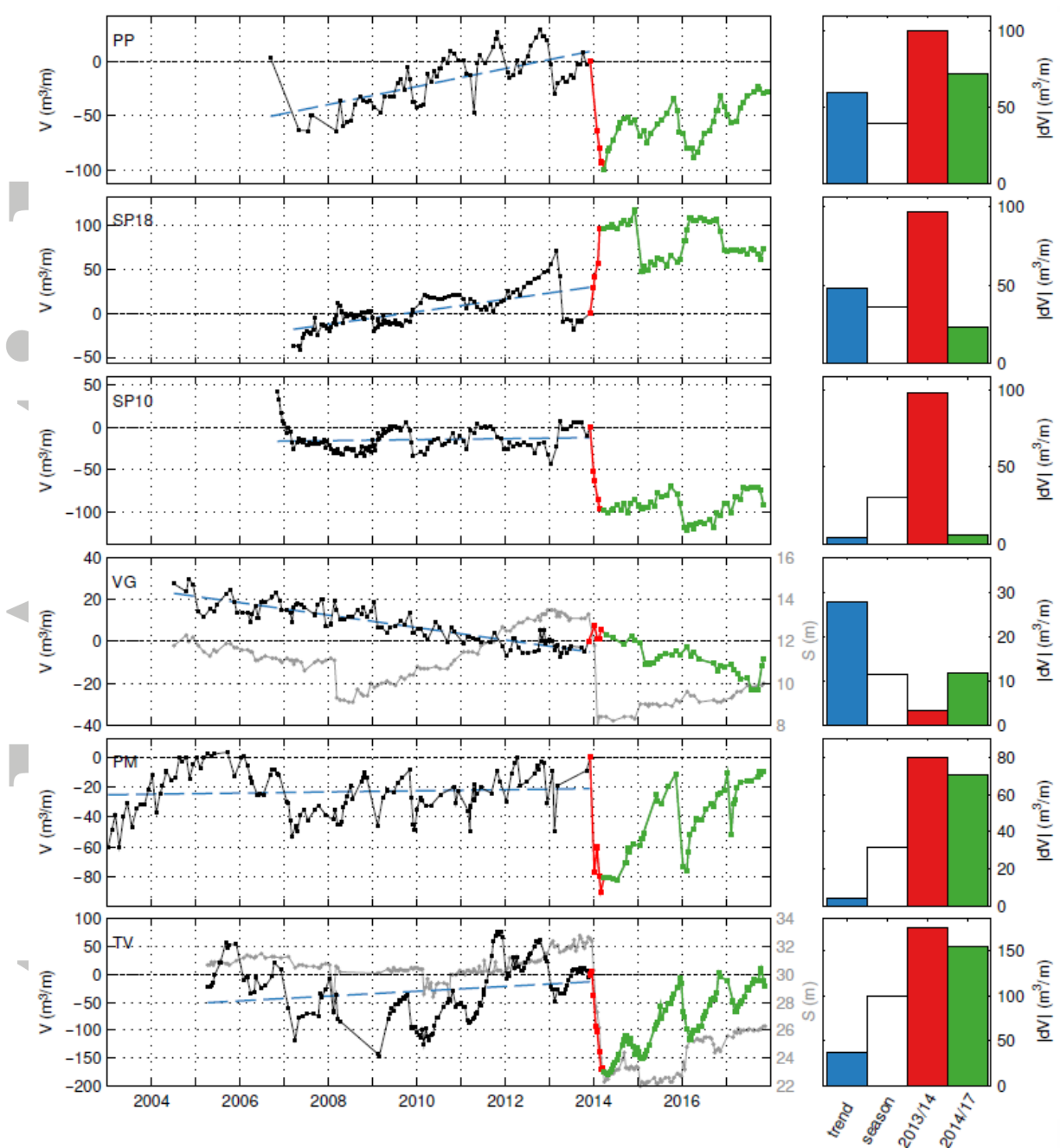
Figure 2. (left) Time series of beach volume at the five study sites (with two profiles shown for Slapton Sands), with the beach volume set to zero on December 1 2013. The dashed blue line represents the long-term trend over the period prior to the 2013/14winter, the red line represents the 2013/14 winter response, and the green line represents the recovery period. For Vougot and Truc Vert the evolution of the location of the dune foot (grey line) is also shown. (right) Absolute values of the volume change associated with the long-term trend (blue), seasonal variability (white), 2013/14 winter response (red), and recovery period (green).
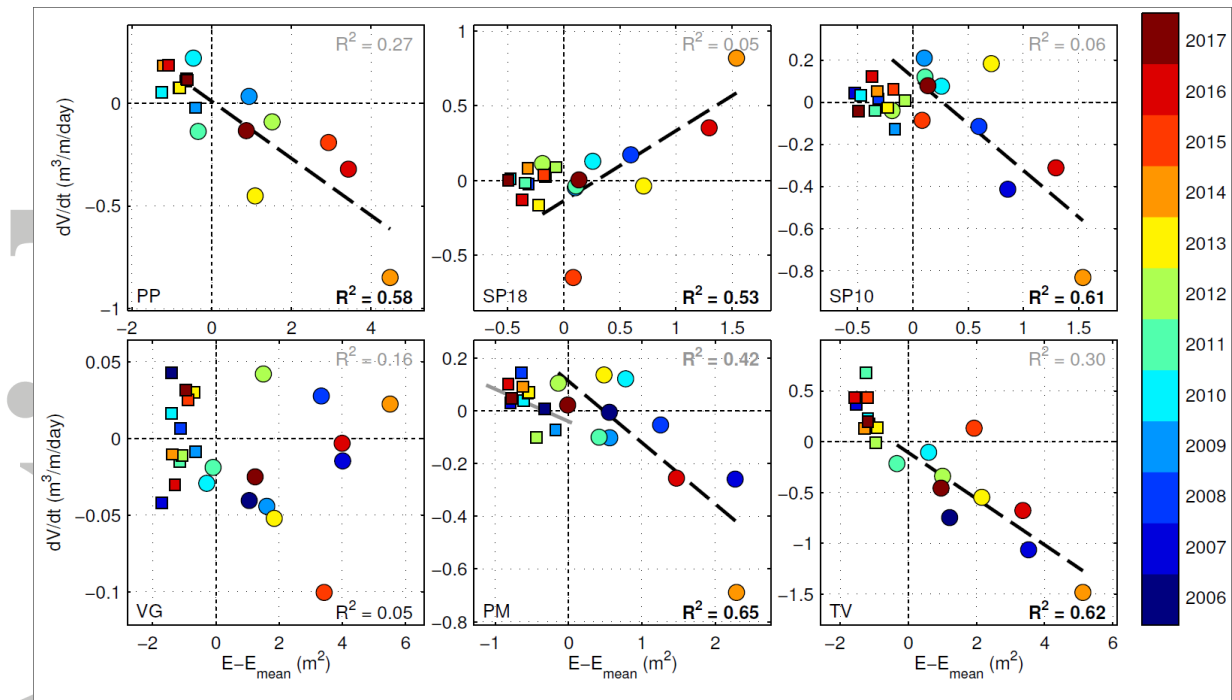
Figure 3. Beach volume changes during winter (circles) and summer-spring-autumn (squares) versus the wave energy anomaly (computed as the deviation of the season-mean wave energy from the long-term (1992–2017) annual mean wave energy), with colors indicating years. The squared correlation coefficients between beach volume changes and wave energy anomaly are given for winter (black) and spring-summer-autumn (grey). Linear regressions for winter (dashed light grey) and summer-spring-autumn (dasheddark grey) are plotted when the correlation is statistically significant at the 95 % level (in that case R^2 is written in bold).
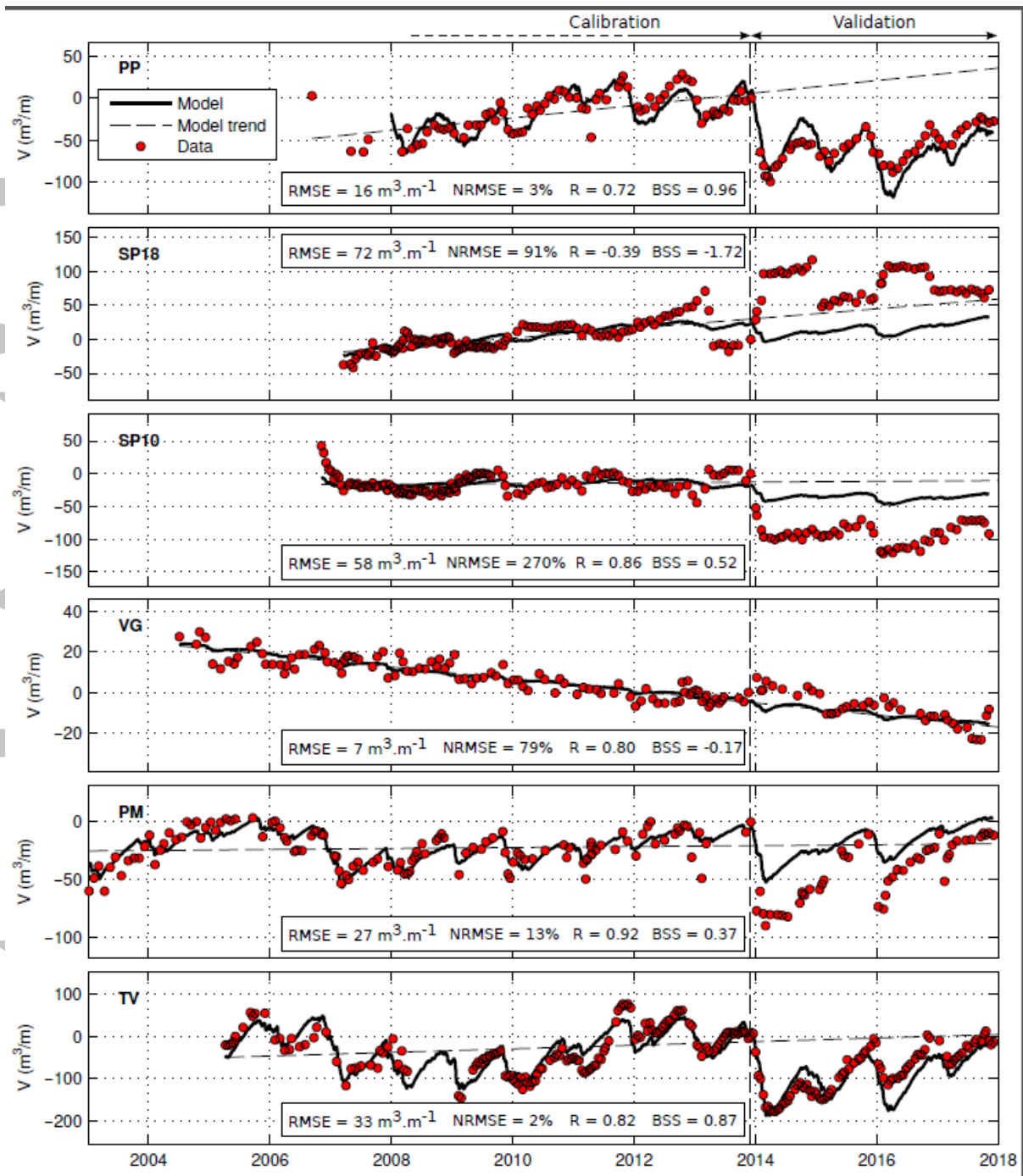
Figure 4. Comparison between ShoreFor model results and observations. Statistical errors are given for the validation period (post-2013/14 winter), and include the root-mean-square error (RMSE), the root-mean-square error normalized by the observed variance (*NRMSE*), the correlation coefficient (*R*) and the Brier Skill Score (*BSS*), with the long-term trend (dash black line) used as the baseline. Note that the calibration period at Perranporth (PP) does not include the four initial measurements, because their low sampling frequency induce error in the model calibration.